http://dx.doi.org/10.5935/0103-5053.20140246

J. Braz. Chem. Soc., Vol. 26, No. 1, 196-208, 2015.
Printed in Brazil - ©2015 Sociedade Brasileira de Química
0103 - 5053 $6.00+0.00

Article

AC-Induced Corrosion of Underground Steel Pipelines. Faradaic Rectification under Cathodic Protection: I. Theoretical Approach with Negligible Electrolyte Resistance

Ibrahim Ibrahim,[a,c] Bernard Tribollet,[b,c] Hisasi Takenouti*[,b,c] and Michel Meyer[d]

[a]*Al-Andalus University, Tartus, Al Qadmus, Syria*

[b]*Laboratoire Interfaces et Systèmes Electrochimique (LISE), Sorbonne Universités, UPMC Univ. Paris 06, UMR 8235, 75005 Paris, France*

[c]*CNRS, UMR 8235, LISE, Case 133, 4 place Jussieu, 75005 Paris, France*

[d]*GDF SUEZ, 361 avenue du Président Wilson, 93211 Saint Denis La Plaine, France*

Tubulações subterrâneas protegidos por um revestimento grosso e por polarização catódica podem sofrer danos externos sérios por corrosão na presença de tensão de corrente alternada (AC) dispersa induzida por sistemas industriais de transporte elétrico de alta tensão, como linhas de tensão ou ferrovias eletrizadas. A origem do aumento da corrosão vem da não-linearidade das características corrente-potencial da interface metal-solo. Neste trabalho, avaliaremos teoricamente o aumento da densidade de corrente de corrosão e o deslocamento de potencial induzido por um sinal AC de alta amplitude a modelos de sistemas sofrendo corrosão: curvas de polarização anódicas obedecendo uma lei exponencial em relação ao potencial, e processo catódico sob a cinética de ativação-difusão mista. A originalidade do presente trabalho se encontra no uso de um número relativamente pequeno de variáveis sem dimensão para descrever a retificação faradaica no deslocamento do potencial e no aumento da corrente de corrosão. Neste artigo, o efeito da resistência do eletrólito foi negligenciado.

Underground pipelines protected with a thick coating and by cathodic polarisation may suffer a serious external corrosion damage in the presence of stray alternating current (AC) voltage induced by high voltage industrial electric transport system, such as power lines or electrified railroads. The origin of the corrosion enhancement comes from the nonlinearity of the current-potential characteristics of the metal-soil interface. In this paper, we will theoretically evaluate the increase of the corrosion current density and the potential shift induced by a high amplitude AC signal to models of corroding systems: anodic polarisation curves obeying an exponential law with respect to the potential, and cathodic process under the mixed activation-diffusion kinetics. The originality of the present work lies in the use of a relatively small number of dimensionless variables to describe the faradaic rectification for the corrosion potential shift and the corrosion current enhancement. In this article, the effect of the electrolyte resistance was neglected.

Keywords: Tafel law, dissolved oxygen reduction, partially diffusion limited kinetics, corrosion potential shift, corrosion current enhancement

Introduction

Focusing the present analysis to the case of the steel/soil interface when the steel is subjected to cathodic protection (CP), a typical situation for coated and buried steel pipelines, it is convenient to start any discussion on alternating current (AC) corrosion mechanism by considering first the state of the CP polarised interface in absence of any AC perturbation. CP is achieved because the cathodic polarisation leads to alkalisation of the soil solution in the near steel surface layer. Then, corrosion protection comes from the precipitation of a protective film consisting, most of the time, of an iron oxide/oxy-hydroxide film having a classical bi-layer structure with a thin compact "passive" inner layer and a thick porous outer layer.[1-5] It is known that AC-induced corrosion on the installations under cathodic protection may significantly threaten their lifetime and safety.[6-22] Despite the numerous laboratory and

*e-mail: hisasi.takenouti@upmc.fr

field studies dedicated to the topic during the last 30 years, there is at present no worldwide consensus on the detailed mechanisms involved in this degradation process.[20,23-26]

AC-enhanced corrosion is a complex phenomenon, due to the periodic excursions, at the fundamental frequency of the AC perturbation, of the steel/soil interfacial potential in a wide range spread over the cathodic and anodic domains, as schematically illustrated in Figure 1a. In this figure, the electrochemical stability of the steel/soil system is illustrated through a simplified Pourbaix diagram in which the span of the excursions of the interfacial potential $E(t)$ is depicted.[27] Figure 1b presents a typical electrical equivalent circuit depicting the local situation at any given coating holiday and adapted from that suggested in the recent state-of-the-art review elaborated by the National Association of Corrosion Engineers (NACE) International Society.[5] These two figures illustrate the correlation between, on one hand, the interfacial potential and, on the other hand, the voltage between the steel and the remote earth resulting from the inductive coupling between the pipeline and the electric power line, as well as the direct current (DC) potential from the steel to the remote earth, resulting from the presence of the CP system.[28]

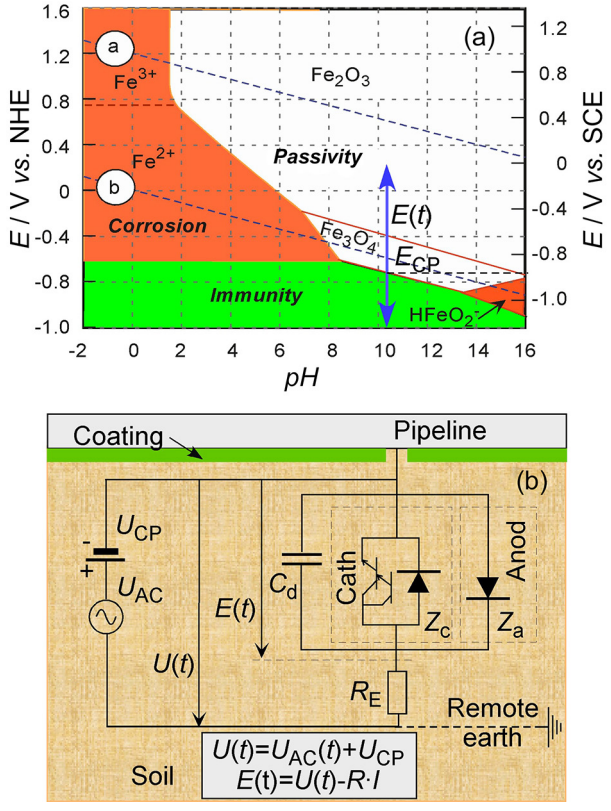

Figure 1. (a) Schematic representation of the potential-pH diagram with potential excursions for a steel electrode under cathodic protection (CP) at E_{CP}, in the presence of AC perturbation $E(t)$; (b) its equivalent electrical circuit with anodic and cathodic contributions by two parallel circuits; anodic reaction with a diode, and cathodic reaction with a diode and a direct current limiter.

In Figure 1a, as it is generally assumed that AC-induced perturbation may be viewed as a "controlled voltage phenomenon", AC perturbation is described as an AC voltage source $E(t)$ superimposed to a DC potential source (E_{CP}). For illustration, the CP potential is set to polarise the steel somewhere between the immunity and the passivity domain.[28]

For the equivalent electrical circuit (Figure 1b), the total current flowing across the interface is, according to the formalism introduced by Taylor and Gileadi,[29] the sum of the capacitive current through the double layer capacitance (C_d) and the faradaic current transferred through the two parallel faradaic circuits. In this circuit, the anodic process is simulated by a simple diode representing an exponential law with respect to the potential and cathodic one by a parallel assembly of a diode and two transistors (for simplified representation of a direct current limiter) representing mixed controlled (activation energy and mass transport control) kinetics. These circuits are then connected to the electrolyte resistance R_E. As a consequence, an ohmic drop through R_E makes the interface potential $E(t)$ smaller than the overall potential $U(t)$.

Due to repetitive excursions in the anodic and cathodic domain, as illustrated in Figure 1a by the arrows, whatever the mechanism, the AC corrosion phenomenon involves coupled interfacial processes leading to chemical changes of the soil solution at the vicinity of the pipe surface at the coating defect. As a first step, these chemical changes consist mainly in "over alkalisation" of the local soil solution, due to cathodic processes stimulated during the cathodic excursions of the electrochemical potential (dissolved oxygen reduction and hydrogen evolution reaction).[21]

Differences in elementary mechanisms, depending on the range of influencing factors occurring in the various actual field situations, may explain why the practical CP criteria, required to safely protect the coated underground steel pipelines against this specific corrosion threat, are still subject to discussion.[1,2,19,30-37]

Another factor influencing the AC corrosion phenomenon is the so-called "faradaic rectification". Since the earlier studies on AC corrosion by Gellings[38] in 1962 then by Bertocci[39] in 1979, it was shown that DC current-potential curves are affected by the presence of AC voltage. In particular, a shift of the corrosion potential (defined as the mean DC interfacial potential for which the mean DC current transferred to the steel/electrolyte interface is zero) and an increase of the corrosion current density (defined as the mean DC anodic - or equivalently cathodic - faradaic current transferred to the interface when the DC interfacial potential is equal to the mean DC

interfacial corrosion potential) are generally observed in presence of AC current. This phenomenon is traditionally named "faradaic rectification".

With respect to the AC corrosion process, three primary factors have a great influence: (*i*) the electrolyte resistance which, because of the $I \times R$ drop, decreases the actual amplitude of the interfacial potential of the AC voltage perturbation; (*ii*) the interfacial capacitance through which a capacitive current will be transferred, which also gives rise the $I \times R$ drop, and consequently decreases the amplitude of the AC voltage perturbation. These two aspects will be treated in part II of this paper, in preparation; (*iii*) under cathodic protection, the electrolyte at the vicinity of the electrode surface may be subject to alkalisation, leading to modifications of the corrosion mechanism and of the electrode kinetics. Actual local pH measurements, together with corrosion tests associated with the mass loss measurements will be reported in part III of this paper.

Faradaic rectification is largely reported in the literature but, for most publications, [23-26,38,39] its effect on the AC corrosion mechanisms was analysed without explicit consideration of the particular situation of cathodically protected interfaces. Besides, the cathodic process will be composed of two reactions, reduction of dissolved oxygen and that of water. When the AC amplitude is high, the range of excursion of the interface potential may be modified, such that the water reduction will be set on. We will emphasise thus the combination of these two phenomena. Particularly, it is intended, in part III of this paper, to highlight the effect of the faradaic rectification phenomenon on the pH evolution of the soil electrolyte at the steel/soil interface, and to study how the alkalisation of the interfacial electrolyte may determine the actual corrosion status of the metal (corrosion protection *vs.* corrosion at the active state).

The aim of the present work is to determine the possible impact of the faradaic rectification effect on the AC corrosion phenomenon in the context of the coated and CP protected underground steel pipelines. To this end, this process is first studied theoretically for different models of the metal/electrolyte interface.

Simplified theoretical approaches are presented in this paper to illustrate the effects of AC perturbation on the electrochemical behaviour of the interface. It ignores the time-related evolution of the interfacial chemistry, namely the surface relaxation phenomena leading to occurrence of inductive or capacitive behaviour. It also ignores the possible alteration of the interfacial kinetics, as well as the triggering of additional electrochemical reactions.

In addition, in the work presented in this first part of the paper, it is assumed that the electrolyte resistance is negligibly small with respect to the interfacial impedance. This is a strong hypothesis, indeed, as will be shown later in this paper, in such case, the interfacial capacitance no longer influences the faradaic rectification effect.

Methodology

Basic expressions on the faradaic rectification for an activation controlled interface

The electrochemical system constituted by the steel/soil electrolyte interface is intrinsically non-linear; therefore the current response induced by a high AC voltage modulation is non-linear, too. If it is assumed that the electrode processes are controlled by the activation energy only, i.e., the interface is obeying the Tafel law, the faradaic current of any electrochemical reaction I_F will follow a generic exponential law with respect to the interfacial potential E. This is often the case for the hydrogen evolution reaction and the anodic dissolution of corroding of metals:

$$I_F = \pm nFK \exp\left[b\left(E - E_{corr,0}\right)\right] = \pm I_{corr,0} \exp\left[b\left(E - E_{corr,0}\right)\right] \quad (1)$$

where ± is according to the conventional sign adopted for the faradaic processes; anodic reactions are expressed as positive and cathodic as negative; b is the activation coefficient or Tafel constant ($\pm\alpha\, n\, F / R\, T$, with the + sign for any anodic reaction and – for any cathodic reaction); α is the transfer or Tafel coefficient between 0 and 1; I_F is the faradaic current; E is the interfacial potential; n, F, R and T are, respectively, the number of electrons exchanged in the reaction, the Faraday constant, the gas constant and the absolute temperature; K is the reaction rate constant; $I_{corr,0}$ is the so called "free" corrosion current density, in the absence of AC perturbation; and $E_{corr,0}$ is the free corrosion potential (also called the open circuit potential).

The symbols and their units are summarised in the Supplementary Information.

It is worth nothing that: (*i*) in the expression above, the reverse reaction was neglected because the potential domain considered in this paper is far from the equilibrium potential of the reactions considered; (*ii*) whatever the nature (anodic or cathodic) of the reaction considered, the so-called "Tafel slope β" is related to the Tafel constant or the kinetic coefficient by the relation:

$$\beta = \frac{\ln(10)}{b} \quad (2)$$

Under AC voltage perturbation, the interfacial potential E will be expressed as:

$$E = E_0 + \Delta E \sin(\omega t) \quad (3)$$

where ω stands for the angular frequency; and ΔE represents the peak-voltage of AC signal. Since the electrolyte resistance R_E is assumed to be negligibly small with respect to the interfacial impedance, the applied potential between the reference and the working electrode U is identical to E.

$$U = E + R_E I \tag{4}$$

If it is assumed that the presence of the AC perturbation does not alter the interfacial medium, then $I_{corr,0}$ will remain the same. The instant faradaic anodic current response can then be expressed by:

$$\begin{aligned} I(t) &= I_{corr,0} \exp\left\{b\left[E_0 + \Delta E \sin(\omega t) - E_{corr,0}\right]\right\} \\ &= I_{corr,0} \exp\left\{b\left[E_0 - E_{corr,0}\right]\right\} \exp\left\{b\Delta E \sin(\omega t)\right\} \end{aligned} \tag{5}$$

where E_0 is the CP polarisation level (= E_{CP}).

By the Taylor expansion of equation 5, around the over-potential ($E_0 - E_{corr,0}$), one gets:

$$I(t) = I_0\left[1 + b\Delta E \sin(\omega t) + \frac{b^2\Delta E^2 \sin^2(\omega t)}{2!} + \frac{b^3\Delta E^3 \sin^3(\omega t)}{3!} + \ldots\right] \tag{6}$$

with $I_0 = I_{corr,0} \exp\left\{b\left(E_0 - E_{corr,0}\right)\right\}$.

The time-averaged faradaic anodic current densities for one entire period of AC signal is given by:

$$\overline{I_F} = \frac{1}{T_0}\int_0^{T_0} I(t)\, dt \tag{7}$$

where T_0 is the entire period of the AC signal.

After mathematical developments described by Lalvani and his group,[40-42] the following expression may be obtained:

$$\overline{I_F} = I_0\left[1 + \sum_1^\infty \frac{b^{2n}\Delta E^{2n}}{2^{2n}(n!)^2}\right] = I_{corr,0} \exp\left\{\left[b\left(E_0 - E_{corr,0}\right)\right]\right\}\left[1 + \sum_1^\infty \frac{b^{2n}\Delta E^{2n}}{2^{2n}(n!)^2}\right] \tag{8}$$

A rigorously identical expression was also derived by Bertocci,[39] using the expansion of the function $\exp\{b\,\Delta E \sin(\omega t)\}$ in a series of products of sines and cosines by the modified Bessel functions of the first kind of order k ($k = 0$ to ∞), $I_{B,k}(z)$, in the form of:

$$\begin{aligned} \exp\left\{z\sin(x)\right\} = I_{B,0}(z) &+ 2\sum_{k=0}^{\infty}(-1)^k I_{B,2k+1}(z)\sin\left\{(2k+1)x\right\} \\ &+ 2\sum_{k=1}^{\infty}(-1)^k I_{B,2k+1}(z)\cos(2kx) \end{aligned} \tag{9}$$

where the modified Bessel functions may be calculated using the following expression:

$$I_{B,n}(z) = \left(\frac{z}{2}\right)^n \sum_{k=0}^{\infty} \frac{\left(\frac{z}{2}\right)^{2k}}{k!(n+k)!} \tag{10}$$

In such development, when calculating the time average value of the faradaic current over one entire period of AC signal ($T_0 = 1/f = 2\pi\ \omega^{-1}$), i.e., the DC component of this current, only the first term of the series, ($I_{B,0}(z)$) is not zero. One can easily observe, from equation 10, that the expression for $I_{B,0}(b\,\Delta E)$ is identical to the corrective term of equation 8. The term $\sum_1^\infty \left[b^{2n}\Delta E^{2n} / \left\{2^{2n}(n!)^2\right\}\right]$ induces the so-called faradaic rectification effect.

Equation 8 shows that the mean faradaic current density is enhanced by the presence of AC perturbation. This effect comes from the faradaic rectification. The faradaic rectification itself is induced by even number harmonics of the current response to the interfacial perturbation. The previous derivation is valid for a sinusoidal perturbation of the interfacial potential. The slope of the $\overline{I_F} = f(E_0)$ curve at E_0 in the presence of AC signal is calculated to be:

$$\left.\frac{\partial \overline{I_F}}{\partial E}\right|_{E=E_0} = bI_{corr,0} \exp\left\{\left[b\left(E_0 - E_{corr,0}\right)\right]\right\}\left[1 + \sum_1^\infty \frac{b^{2n}\Delta E^{2n}}{2^{2n}(n!)^2}\right] \tag{11}$$

The complete corrosion process, including the anodic and cathodic processes, is now considered. If no interaction between the two processes is assumed, the mean faradaic current is the sum of the mean anodic and cathodic currents. The following three reactions can be taken into account; the one for the anodic process relative to the dissolution of metal is:

$$Fe \rightarrow Fe^{2+} + 2e^- \tag{12}$$

The two others are the cathodic processes relative to the reduction of water and that of dissolved oxygen:

$$2H_2O + 2e^- \rightarrow H_2 + 2OH^- \tag{13}$$

$$O_2 + 2H_2O + 4e^- \rightarrow 4OH^- \tag{14}$$

The reduction of dissolved oxygen is more common in the corrosion process in weakly acidic to alkaline media containing dissolved oxygen. This reaction is generally controlled by mixed kinetics, i.e., coupling of the activation energy and the mass transport processes. For sake of simplicity, we will call it the "mixed corrosion mechanism" when coupled with the anodic process. In contrast, when the corrosion process is controlled by anodic dissolution and water reduction, both following the exponential law with respect to the potential, it will be called "bi-tafelian

corrosion mechanism". This corrosion mechanism may take place in an acidic medium. When the anodic reaction obeying the Tafel law is coupled with two cathodic reactions, this corrosion mechanism will be named "three reaction corrosion mechanism".

The effect of a high amplitude AC signal on the corroding metal around the open circuit potential with bi-tafelian or the mixed corrosion mechanisms are largely reported in the literature.[38-45] However, as far as we know, no theoretical approach of faradaic rectification on the AC-induced corrosion with the three reaction corrosion mechanism under CP system has yet been reported.

Modelling of the faradaic rectification in the solution containing dissolved oxygen and in negligibly small electrolyte resistance

For equations 12 and 13, the reaction rates are considered to obey the Tafel law, therefore one can write the following equations, according to the generic equation 1 presented above:

$$I_a = I_{corr,0} \exp\left\{b_a \left(E - E_{corr,0}\right)\right\} \quad (15)$$

$$I_{c,H_2O} = -I_{corr,0,H_2O} \exp\left\{b_{c,H_2O} \left(E - E_{corr,0}\right)\right\} \quad (16)$$

where $I_{corr,0}$ is the "free" corrosion current density in the absence of AC perturbation. For a cathodic reaction, $I_{corr,0,H_2O}$ represents the part of the water reduction to the overall corrosion current density. Note that, in the presence of only one anodic reaction, as it is the case anyhow in this paper, and if only water reduction as a cathodic process is taking place simultaneously, then $I_{corr,0,H_2O} = I_{corr,0}$.

For the reduction of dissolved oxygen, the reaction rate will be, in most practical situations, controlled partly by the diffusion process, and expressed by the classical Butler-Volmer expression in the form of (see for instance[43]):

$$I_{c,O_2}(E) = n_{c,O_2} F K_{c,O_2} [O_2]_{int} \exp\left\{-\frac{\alpha_{c,O_2} F}{RT}(E - E^0_{c,O_2})\right\} \quad (17)$$

where K_{c,O_2} is the rate constant of the cathodic oxygen reduction process; $[O_2]_{int}$: is the interfacial concentration of dissolved oxygen, at the interfacial potential E; E^0_{c,O_2} is the standard equilibrium potential of the dissolved oxygen/OH^- redox couple; α_{c,O_2} is the transfer coefficient of the reduction process; and n_{c,O_2} is the number of electrons involved in the elementary reduction process, here equal to 4.

If $I_{corr,0,O_2}$ is the partial cathodic current density of the dissolved oxygen reduction, and contributing to the total "free corrosion current density", $I_{corr,0}$, we can also apply the generic expression above for the case where $E = E_{corr,0}$ and express it as:

$$I_{corr,0,O_2} = n_{c,O_2} F K_{c,O_2} [O_2]_{corr,0} \exp\left\{-\frac{\alpha_{c,O_2} F}{RT}(E_{corr,0} - E^0_{c,O_2})\right\} \quad (18)$$

where $[O_2]_{corr,0}$ is the interfacial concentration of dissolved oxygen at the free corrosion potential, $E_{corr,0}$.

Combining equations 17 and 18, and defining b_{c,O_2}, the kinetic coefficient, or Tafel constant, for the cathodic reduction of dissolved oxygen as:

$$b_{c,O_2} = -\frac{\alpha_{c,O_2} F}{RT} \quad (19)$$

we obtain:

$$I_{c,O_2} = -I_{corr,0,O_2} \frac{[O_2]_{int}}{[O_2]_{corr,0}} \exp\left\{b_{c,O_2}(E - E_{corr,0})\right\} \quad (20)$$

Under AC voltage perturbation of the interfacial potential $E(t)$ (equation 3), the total faradaic current density will be expressed by the sum of the three faradaic currents contributing to the overall electrochemical process (equations 15, 16 and 20). Consequently, assuming that the three elementary faradaic currents are independent of one another, the total instant faradaic current density transferred through the interface may by expressed as the sum of the three individual time-dependent faradaic current densities:

$$\begin{aligned} I(t) = {} & I_{corr,0} \exp\left\{b_a\left[E_0 - E_{corr,0} + \Delta E \sin(\omega t)\right]\right\} \\ & - I_{corr,0,O_2} \frac{[O_2]_{int}}{[O_2]_{corr,0}} \exp\left\{b_{c,O_2}\left[E_0 - E_{corr,0} + \Delta E \sin(\omega t)\right]\right\} \\ & - I_{corr,0,H_2O} \exp\left\{b_{c,H_2O}\left[E_0 - E_{corr,0} + \Delta E \sin(\omega t)\right]\right\} \end{aligned} \quad (21)$$

Note that, upon hypothesis of mutual independency of the faradaic currents, the overall "free corrosion current density" $I_{corr,0}$ results in the sum of the two partial cathodic current contributions at $E_{corr,0}$. We can write the fractional contribution of the water reduction to the total free corrosion current as:

$$\lambda_{H_2O} = \frac{I_{corr,0,H_2O}}{I_{corr,0}} \quad (22)$$

where λ_{H_2O} is a positive coefficient smaller than 1. If λ_{H_2O} is zero, no water reduction is taking place (mixed corrosion mechanism) and if $\lambda_{H_2O} = 1$, the whole cathodic reaction is the water reduction (bi-tafelian corrosion mechanism).

Then, the total instant faradaic current density is expressed by:

$$I_F(t) = I_{corr,0}\begin{bmatrix} \exp\left\{b_a\left[E_0 - E_{corr,0} + \Delta E\sin(\omega t)\right]\right\} \\ -\left(1-\lambda_{H_2O}\right)\dfrac{[O_2]_{int}}{[O_2]_{corr,0}}\exp\left\{b_{c,O_2}\left[E_0 - E_{corr,0} + \Delta E\sin(\omega t)\right]\right\} \\ -\lambda_{H_2O}\exp\left\{b_{c,H_2O}\left[E_0 - E_{corr,0} + \Delta E\sin(\omega t)\right]\right\} \end{bmatrix} \quad (23)$$

The time-averaged $\overline{I_F}$ for the entire period of AC signal is then given by:

$$\overline{I_F} = \overline{I_a} + \overline{I_{c,O_2}} + \overline{I_{c,H_2O}} = \frac{1}{T_0}\int_0^{T_0}\left[I_a(t) + I_{c,O_2}(t) + I_{c,H_2O}(t)\right]dt \quad (24)$$

where $I_{c,O_2}(t)$ is given by:

$$I_{c,O_2}(t) = -I_{corr,0,O_2}\frac{[O_2]_{int}(t)}{[O_2]_{corr,0}}\exp\left\{b_{c,O_2}\left[E_0 - E_{corr,0} + \Delta E\sin(\omega t)\right]\right\} \quad (25)$$

In this equation, the interfacial concentration of dissolved oxygen may theoretically be split into the sum of a constant component and a variable component, periodically varying at the AC perturbation frequency, both depending on E_0 and on the variables associated with the AC perturbation, i.e., ΔE and ω.

However, according to our current laboratory experience, the frequency of AC perturbation coming from currently operating industrial equipment (typically 16.67, 50, or 60 Hz) is generally too high to lead to a significant concentration modulation of dissolved oxygen at the vicinity of the electrode. Then, it is assumed that the $[O_2]_{int}$ induced by AC signal remains constant. The instant cathodic faradaic current $I_{c,O_2}(t)$ can then be written as:

$$I_{c,O_2}(t) = -I_{corr,0,O_2}\frac{[O_2]_{int}(E_0)}{[O_2]_{corr,0}}\exp\left\{b_{c,O_2}\left[E_0 - E_{corr,0} + \Delta E\sin(\omega t)\right]\right\} \quad (26)$$

The right hand side of this equation will be developed by the expansion of $\exp\{b_{c,O_2}\,\Delta E\sin(\omega t)\}$ into a series of products of sines and cosines by the modified Bessel functions, as proposed by Bertocci.[39] Then, by integrating the equation over one period of AC perturbation, the time-averaged cathodic faradaic current of the oxygen reduction reaction $\overline{I_{c,O_2}}$ is expressed by:

$$\overline{I_{c,O_2}} = -I_{corr,0,O_2}\frac{[O_2]_{int}(E_0)}{[O_2]_{corr,0}}\exp\left\{b_{c,O_2}\left[E_0 - E_{corr,0}\right]\right\}I_{B,0}\left(b_{c,O_2}\Delta E\right) \quad (27)$$

where the term $I_{B,0}(z)$ with $z = b_{c,O_2}\,\Delta E$ symbolically represents the first kind modified Bessel function of order 0 of the variable z.

Upon the hypothesis adopted here, i.e., the interfacial dissolved oxygen concentration is constant and equal to the steady state dissolved oxygen concentration at the mean DC potential, E_0, the mean faradaic DC cathodic current density can be related to the mass flux towards the steel surface of oxygen Φ_{O_2} by:

$$\overline{I_{c,O_2}} = I_{c,O_2}(E_0) = n_{c,O_2}F\Phi_{O_2}(E_0) \quad (28)$$

Applying the Nernst diffusion layer theory, this current density will also be expressed by:

$$\overline{I_{c,O_2}} = I_{c,O_2}(E_0) = -\frac{n_{c,O_2}FD_{O_2}\left\{[O_2]_\infty - [O_2]_{int}(E_0)\right\}}{\delta} \quad (29)$$

where $[O_2]_\infty$ is the bulk concentrations of dissolved oxygen; D_{O_2} is the diffusion coefficient of dissolved oxygen; and δ is the thickness of the diffusion layer, assumed to be constant.

At the diffusion limited plateau, the diffusion limiting current density I_{lim,O_2} is obtained for the interfacial concentration $[O_2]_{int} = 0$, then, we yield:

$$I_{lim,O_2} = -\frac{n_{c,O_2}FD_{O_2}[O_2]_\infty}{\delta} \quad (30)$$

Combination of equations 29 and 30 gives:

$$[O_2]_{int}(E_0) = [O_2]_\infty\left(1 - \frac{I_{c,O_2}(E_0)}{I_{lim,O_2}}\right) = [O_2]_\infty\left(1 - \frac{\overline{I_{c,O_2}}}{I_{lim,O_2}}\right) \quad (31)$$

A similar relationship for the underground steel tube/soil interface, i.e., at the free corrosion potential $E_{corr,0}$ can be derived. However, one must take account that, in this document, by convention, a positive sign is chosen for the corrosion currents, hence I_{corr,O_2} is positive, whereas the sign for the cathodic current I_{lim,O_2} is negative. Consequently, there is an opposite sign in the expression in brackets in the right hand side of the equation equivalent to equation 31 at the free corrosion potential, so that we get:

$$[O_2]_{corr,0} = [O_2]_\infty\left(1 + \frac{I_{corr,0,O_2}}{I_{lim,O_2}}\right) \quad (32)$$

Reporting equations 31 and 32 into the expression of the mean DC current density $\overline{I_{c,O_2}}$ (equation 27), we obtain:

$$\overline{I_{c,O_2}} = -I_{corr,0,O_2}\frac{\left[1 - \dfrac{\overline{I_{c,O_2}}}{I_{lim,O_2}}\right]}{\left[1 + \dfrac{I_{corr,0,O_2}}{I_{lim,O_2}}\right]}\exp\left\{b_{c,O_2}\left[E_0 - E_{corr,0}\right]\right\}I_{B,0}\left(b_{c,O_2}\Delta E\right) \quad (33)$$

Rearranging this expression, we get:

$$\overline{I_{C,O_2}} = -\frac{I_{corr,0,O_2}\exp\left\{b_{c,O_2}\left[E_0 - E_{corr,0}\right]\right\} I_{B,0}\left(b_{c,O_2}\Delta E\right)}{\left[1+\frac{I_{corr,0,O_2}}{I_{lim,O_2}} - \left(\frac{I_{corr,0,O_2}}{I_{lim,O_2}}\right)\exp\left\{b_{c,O_2}\left[E_0 - E_{corr,0}\right]\right\} I_{B,0}\left(b_{c,O_2}\Delta E\right)\right]} \quad (34)$$

Note that this equation is similar to that derived by Nagy and Thomas,[43] if one takes into account the convention adopted here for the sign of cathodic processes. As pointed out by these authors, the equation is completely general, because it describes the oxygen reduction process under mass transport control ($-I_{lim,O_2} = I_{corr,0,O_2}$), mixed control ($-I_{lim,O_2} > I_{corr,0}$), or charge transfer control ($I_{lim,O_2} = -\infty$, i.e., $I_{corr,0,O_2} / I_{lim,O_2} = 0$).

To get the time-averaged total faradaic current for the entire period of AC signal, the two other terms (the anodic oxidation of metal and the cathodic reduction of water) of equation 24 shall be now considered. Adding the three time-averaged faradaic currents, and using the same formalism as in equation 27, the time-averaged total faradaic current for the entire period of AC signal, $\overline{I_F}$ is expressed by:

$$\overline{I_F} = I_{corr,0}\begin{bmatrix} \exp\left\{b_a\left(E_0 - E_{corr,0}\right)\right\} I_{B,0}\left(b_a\Delta E\right) \\ -\left(1-\lambda_{H_2O}\right)\dfrac{\exp\left\{b_{c,O_2}\left(E_0 - E_{corr,0}\right)\right\} I_{B,0}\left(b_{c,O_2}\Delta E\right)}{D_t} \\ -\lambda_{H_2O}\exp\left\{b_{c,H_2O}\left(E_0 - E_{corr,0}\right)\right\} I_{B,0}\left(b_{c,H_2O}\Delta E\right) \end{bmatrix} \quad (35)$$

where the determinant D_t is:

$$D_t = 1 + \frac{\left(1-\lambda_{H_2O}\right)I_{corr,0}}{I_{lim,O_2}} - \left(\frac{\left(1-\lambda_{H_2O}\right)I_{corr,0}}{I_{lim,O_2}}\right)\exp\left\{b_{c,O_2}\left(E_0 - E_{corr,0}\right)\right\} I_{B,0}\left(b_{c,O_2}\Delta E\right) \quad (36)$$

In this equation, λ_{H_2O} represents, as defined in equation 22, the contribution of the water reduction to the total free corrosion current.

The interest of this equation is to explicitly describe, through the three modified Bessel functions of the first kind $I_{B,0}(z)$ with $z = b_a\,\Delta E$, $b_{c,O_2}\,\Delta E$, and $b_{c,H_2O}\,\Delta E$, the effect of AC perturbation on the mean DC polarisation curve, need to be numerically calculated. This development is basically similar to that carried out by Bosch and Bogaerts.[44]

This development shows that another parameter is necessary to completely define the electrochemical behaviour of the corroding electrode with both water and dissolved oxygen reduction reactions; the ratio of the diffusion limiting current density of the dissolved oxygen reduction over the total free corrosion current density (r_{diff,O_2}); "–" sign is added such that this parameter is positive:

$$r_{diff,O_2} = -\frac{\left(1-\lambda_{H_2O}\right)I_{corr,0}}{I_{lim,O_2}} \quad (37)$$

If this parameter is equal to 1, the oxygen reduction is under pure mass transport (diffusion) control, whereas when the oxygen reduction kinetics is mainly controlled by the activation energy, this parameter will be represented by a very small positive value (the corrosion current density markedly smaller than the diffusion limiting current density). Now, we will perform the simulation calculations of the faradaic rectification and its effect on the corrosion kinetics under cathodic protection.

Digital simulations

As for the cathodic processes, we will separate two cases for simulation calculations; first taking into consideration the reduction of dissolved oxygen partly controlled by the diffusion (mixed corrosion mechanism), and then two reactions, the reduction of dissolved oxygen and that of water, hydrogen evolution reaction (three reaction corrosion mechanism). The case where the cathodic reaction merely consists in the reduction of water, following the Tafel law (bi-tafelian corrosion mechanism), will be shown for comparison.

The DC mean current density *vs*. DC mean interfacial potential, in other terms, the DC polarisation curve with the corrosion current enhancement induced by the AC voltage perturbation ΔE, was computed, using equation 35 together with symbolic manipulation and numerical computation using the Mathematica software.[46]

With equation 35, the effect of AC voltage on the polarisation curves was calculated for different peak-voltages. For this calculation, the corrosion kinetic constants used are as listed in Table 1.

The results of the simulation calculation are presented in Figure 2.

In this figure, with corrosion kinetic parameters values often observed experimentally, it is observed that the mean faradaic current density $\overline{I_F}$ for both anodic and cathodic branches increases in the presence of AC perturbation. A "pseudo-plateau", where the DC current is partially limited by the oxygen mass transport, can be seen on the unperturbed

Table 1. Corrosion kinetic parameters used for the simulation calculations

Items	$E_{corr,0}$ / V	$I_{corr,0}$ / (μA cm^{-2})	b_a / V^{-1}	b_{c,O_2} / V^{-1}	b_{c,H_2O} / V^{-1}	λ_{H_2O}	r_{diff,O_2}
	–0.7	20	38.4	–12.8	–12.8	0.1	0.3

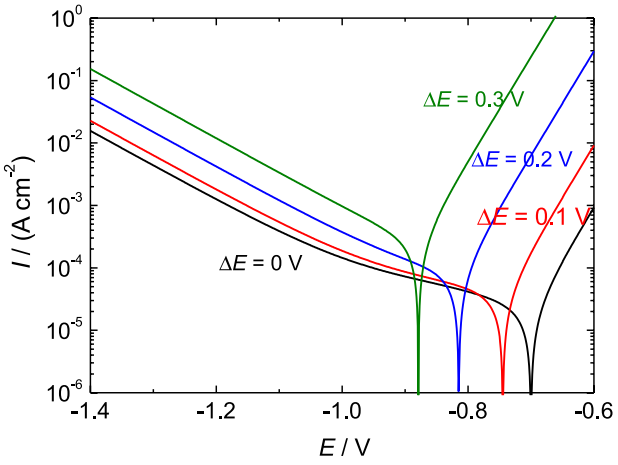

Figure 2. Mean DC current density $\overline{I_F}$-E curves under AC perturbation for the three reaction mechanism, and with negligible solution resistance. Kinetic constants displayed in Table 1.

DC polarisation curve, for the set of kinetics parameters used here. Besides, one salient point to be emphasised is that this current plateau becomes narrower with increasing ΔE values. When the activation energy of the anodic process is higher than that of the cathodic ones ($b_a + b_c > 0$), and in agreement with experimental data or theoretical analyses reported by many authors,[39-44] the corrosion potential in the presence of AC signal shifts towards more a negative direction. It may worth to recall that when R_E is negligibly small, the mean DC potential E is not modified by AC perturbation, since this signal is sinusoidal under potential regulation. It is also worth recalling that the kinetic constants used correspond to the corrosion of iron in active state, since the corrosion of the pipeline may take place by pitting, and in this situation, the corrosion process may take place likely as the active dissolution of iron.

Results and Discussion

Cathodic reaction by the reduction of dissolved oxygen by mixed kinetics

At first, a system with only one cathodic reaction, oxygen reduction under mixed control of diffusion process, was considered to illustrate the primary effect of the mass transport limitation on the shift of the corrosion potential and the enhancement of corrosion current density. This corrosion model corresponds to the case where $\lambda_{H_2O} = 0$.

Several dimensionless entities were introduced to generalise the output results of the digital simulations as much as possible.

The dimensionless corrosion potential shift $<E_{corr,AV}>$ with respect to the free corrosion potential in the presence of the alternating voltage perturbation is expressed as follows:

$$< E_{corr,AV} > = \frac{E_{corr,AV} - E_{corr,0}}{\Delta E} \quad (38)$$

where $E_{corr,AV}$ is the corrosion potential in the presence of the alternating voltage perturbation, which is defined as the mean (DC) interfacial potential for which the overall (external) mean (DC) faradaic current $\overline{I_F}$ is zero.

The enhancement of the corrosion current density is expressed in the reduced scale by:

$$< I_{corr,AV} > = \frac{I_{corr,AV}}{I_{corr,0}} \quad (39)$$

where $I_{corr,AV}$, the corrosion current density in presence of the alternating voltage perturbation, is equal to the mean (DC) faradaic anodic current density (or, equivalently, cathodic, insofar as these two currents have equal values at this potential) at the interfacial potential $E_{corr,AV}$, for the given AC perturbation ΔE.

The peak-voltage of AC perturbation ΔE is normalised as follows.

$$< \Delta E > = \frac{\Delta E}{R_p I_{corr,0}} \quad (40)$$

In this equation R_p, the polarisation resistance, is the slope of the I-E curve, in the absence of any AC perturbation, at the open circuit potential, which is defined as follows:

$$\frac{1}{R_p} = \left.\frac{dI_F}{dE}\right|_{E=E_{corr,0}} \quad (41)$$

Using this definition and equation 35, with ΔE set to 0, the polarisation resistance for the model of interface without the water reduction reaction ($\lambda_{H_2O} = 0$) can be expressed by:

$$\frac{1}{R_p} = I_{corr,0}\left[b_a - \left(1 - r_{diff,O_2}\right) b_{c,O_2}\right] \quad (42)$$

To obtain especially the effect of Tafel constants on $<E_{corr,AV}>$ and $<I_{corr,AV}>$, the ratio of b_a and b_{c,O_2} is defined as follows:

$$r_{O_2/a} = -\frac{b_{c,O_2}}{b_a} \quad (43)$$

Here, the subscript "a" represents the anodic reaction. Since b_c is negative, the $r_{O_2/a}$ value is positive. When the two Tafel constants are equal in absolute value, then, $r_{O_2/a} = 1$.

Results of the simulation calculation on the corrosion potential shift are presented in Figure 3. For comparison, the corrosion potential shift of the bi-tafelian corrosion mechanism, the case most often reported in the literature, is overlaid as dashed lines in Figure 3.

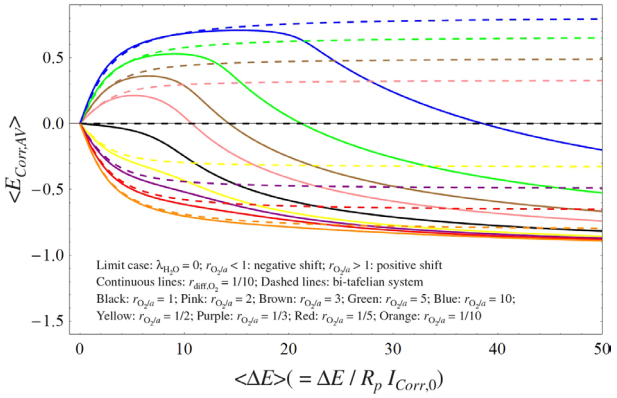

Figure 3. Effect of $r_{O_2/a}$ and $<\Delta E>$ on the reduced shift of corrosion potential $<E_{corr,AV}>$ for the mixed corrosion mechanism. A small diffusion component at $E_{corr,0}$ ($r_{diff,O_2} = 0.1$), with negligible electrolyte resistance. $r_{O_2/a}$ values from top to bottom: blue = 10, green = 5, brown = 3, pink = 2, black = 1, yellow = 0.5, purple = 1/3, red = 0.2, and orange = 0.1.

The solid line curves show the variation of the normalised (dimensionless) corrosion potential shift $<E_{corr,AV}>$ *vs.* $<\Delta E>$ for the mixed corrosion mechanism. In this figure, the ratio of the total free corrosion current density to the diffusion limiting current density of the dissolved oxygen reduction reaction is set to $r_{diff,O_2} = 0.1$ at $E_{corr,0}$. In other terms, the dissolved oxygen reduction is weakly controlled by the diffusion of oxygen towards the surface, at the free corrosion potential in the absence of AC perturbation. A series of curves are plotted for various $r_{O_2/a}$ ratios. It can be noticed that this weak mass transport limitation modifies significantly the normalised corrosion potential shift as a function of the dimensionless amplitude. One can observe that for $r_{O_2/a} < 1$, the corrosion potential shifts towards a more negative direction with respect to the corrosion potential of the non-perturbed interface. This potential shift is greater for the mixed kinetics compared with the bi-tafelian system (dashed curves). Conversely, for $r_{O_2/a} > 1$, the corrosion potential shifts towards a more anodic direction, but this potential shift is smaller compared with the corresponding curve for the bi-tafelian corrosion mechanism. This decrease significantly grows with the increase of the $<\Delta E>$ ratio, such that, at high values of this ratio, the shift becomes negative and tends, for the higher values of this ratio, toward the negative shift of the corresponding bi-tafelian system having a $r_{O_2/a}$ lower than 1. As can be seen in Figure 2, the apparent local Tafel constant b_c becomes smaller, thus the local $r_{O_2/a}$ becomes even smaller than 1. Under CP, the cathodic reaction may be controlled by the diffusion of dissolved oxygen, therefore the presence of high AC perturbing signal may lead to an over protection.

Figure 4 presents a similar curve where r_{diff,O_2} is even smaller, i.e., equal to 0.01. It is observed that, in this case, only at relatively high values of the $<\Delta E>$, similar effects on $<E_{corr,AV}>$ appear on the dimensionless corrosion potential shift $<E_{corr,AV}>$. In addition, in this figure, the case where the cathodic reaction is entirely controlled by the diffusion process ($r_{diff,O_2} = 1$) is also shown. It can be remarked that, in this case, $<E_{corr,AV}>$ is no longer depending on the $r_{O_2/a}$ ratio. Indeed, in this case, the cathodic process controls entirely the mean DC response of the interface to the AC perturbation, in the cathodic domain, up to the free corrosion potential $E_{corr,0}$. The cathodic current density *vs.* potential is thus parallel to the potential axis, and apparent b_c is zero. It is noteworthy that the value of $R_p I_{corr,0}$ is about 0.02 V for the majority of cases for corrosion in the active state. So, $<\Delta E> = 50$ corresponds to the peak-voltage ΔE of 1 V.

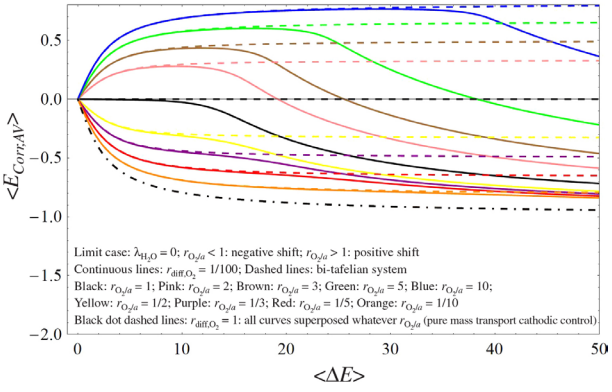

Figure 4. Similar curves to Figure 3, but $r_{diff,O_2} = 0.01$. The curves for various $r_{O_2/a}$ are represented as Figure 3. The dot-dashed curve at the most bottom position represents $r_{diff,O_2} = 1$ (cathodic kinetics entirely controlled by the diffusion).

Figure 5 presents the variation of $<I_{corr,AV}>$ with respect to the dimensionless peak voltage $<\Delta E>$ at conditions similar to Figure 3. In this figure, the reduction of dissolved oxygen is partly limited by the diffusion, $r_{diff,O_2} = 0.1$ at $E_{corr,0}$. In the same figure, the case of bi-tafelian corrosion mechanism is also presented with dashed lines. It can be observed that this mildly mass transport limitation decreases significantly the relative enhancement of the corrosion current induced by AC perturbation, for any given value of $<\Delta E>$. Besides, in any case, at high $<\Delta E>$, the enhancement of the corrosion current tends toward the limit equal to $1/r_{diff,O_2}$. When the amplitude of the excursions increases greatly, $<\Delta E>$ also increases, such that $<I_{corr,AV}>$ will be determined only by the cathodic diffusion limiting current density.

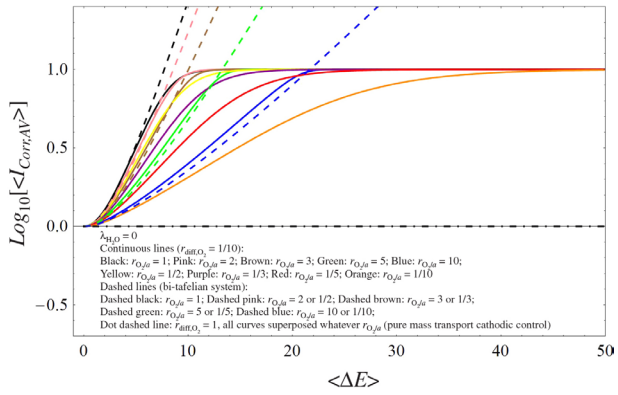

Figure 5. Relative enhancement of the corrosion current (solid lines), for the same system as Figure 3, $r_{\mathrm{diff},O_2} = 0.1$ with negligible electrolyte resistance. Comparison with a bi-Tafelian corrosion mechanism shown as dashed curves. For $r_{\mathrm{diff},O_2} = 1$ (cathodic kinetics entirely controlled by the diffusion), shown as a dot-dashed curve, no effect of $<\Delta E>$ is observed.

The case of a pure diffusion control of the oxygen reduction is also represented in this Figure 5. In this situation, the corrosion current density is determined solely by the diffusion limiting current. Since the current is independent of the potential, there is no longer the faradaic rectification effect, consequently, no enhancement of the corrosion current occurs, whatever the values of the $r_{O_2/a}$ and $<\Delta E>$.

Cathodic process composed of the reduction of dissolved oxygen and that of water

In the section above, the effect of AC perturbation on the corrosion model constituted of the metal dissolution obeying the Tafel law and the cathodic reaction with mixed diffusion kinetics was examined. Now, we will analyse the faradaic rectification effect for the three reaction corrosion mechanism, i.e., in the case where the cathodic current is composed of two contributions, the mixed diffusion kinetics representing the reduction of dissolved oxygen and the tafelian characteristics corresponding to the water reduction in parallel to the active anodic dissolution obeying the Tafel law. As illustrated in Figure 2, in absence of AC voltage and at the potential domain close to the open circuit one, the cathodic current is essentially determined by the reduction of dissolved oxygen, whereas the water reduction reaction determines the overall cathodic current at higher cathodic potentials.

The faradaic current density of the three reaction mechanism is expressed by equation 35. In this case, the polarisation resistance is expressed by the following equation instead of equation 42:

$$\frac{1}{R_p} = I_{\mathrm{corr},0}\left[b_a - \lambda_{H_2O} b_{c,H_2O} - \left(1-\lambda_{H_2O}\right)\left(1-r_{\mathrm{diff},O_2}\right) b_{c,O_2}\right] \quad (44)$$

The following ratio of the kinetic coefficients is now introduced for the sake of generalisation of simulation calculation results:

$$r_{H_2O/a} = -\frac{b_{c,H_2O}}{b_a} \quad (45)$$

This equation is similar to equation 43 for the reduction of dissolved oxygen.

The presence of a second reduction reaction, the water reduction, together with the oxygen reduction, modifies significantly the variation of both the normalised corrosion potential shift and the relative corrosion current enhancement as a function of $<\Delta E>$. Figure 6 shows the relative corrosion potential shift $<E_{\mathrm{corr,AV}}>$ *vs.* $<\Delta E>$. For digital simulations, the Tafel constants b_{c,O_2} and $b_{c,H_2O,}$ are set to the same value, i.e., $r_{O_2/a} = r_{H_2O/a}$. It is observed that when the water reduction reaction is involved, these curves exhibit the behaviour observed above for relatively small $<\Delta E>$, but they approach asymptotically to the bi-tafelian case, when the second cathodic reduction reaction is involved, particularly at high $<\Delta E>$ values.

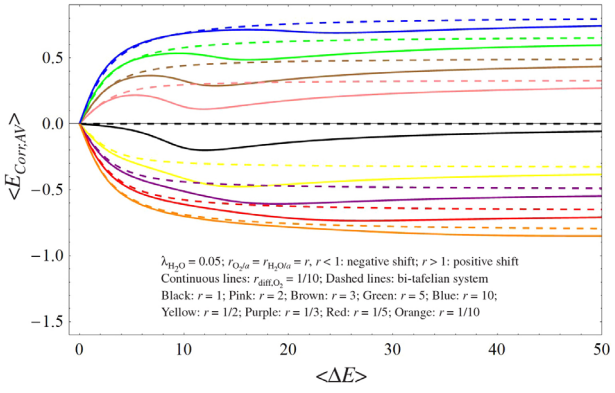

Figure 6. Effect of $r_{O_2/a}$ (or $r_{H_2O/a}$), and $<E_{\mathrm{corr,AV}}>$ with respect to $<\Delta E>$, for a three reaction corrosion mechanism. The water reduction contribution to the total cathodic faradaic current is minor ($\lambda_{H_2O} = 0.05$), and the oxygen reduction reaction is characterised by a small diffusion contribution ($r_{\mathrm{diff},O_2} = 0.1$) at $E_{\mathrm{corr},0}$. Electrolyte resistance R_E is neglected. Comparison with a bi-Tafelian corrosion mechanism is shown as dashed lines. The Tafel constant ratio r supplies different curves, which are distinguished as indicated in Figure 3.

Figure 7 displays $<I_{\mathrm{corr,AV}}>$ *vs.* $<\Delta E>$ curves under AC perturbation. It can be remarked that, compared with the case of the mixed corrosion mechanism, even for relatively small value of λ_{H_2O} (= 0.05), that is to say, even though the water reduction reaction is a minor cathodic component around the free corrosion potential, the presence of this reduction reaction deeply modifies the $<I_{\mathrm{corr,AV}}>$ *vs.* $<\Delta E>$ curves. No limit of $<I_{\mathrm{corr,AV}}>$ is observed here in contrast to Figure 5 for the mixed corrosion mechanism. For the

three reaction mechanism, and for small <Δ*E*> values, the corrosion current enhancement is smaller than in the case of the mixed corrosion mechanism.

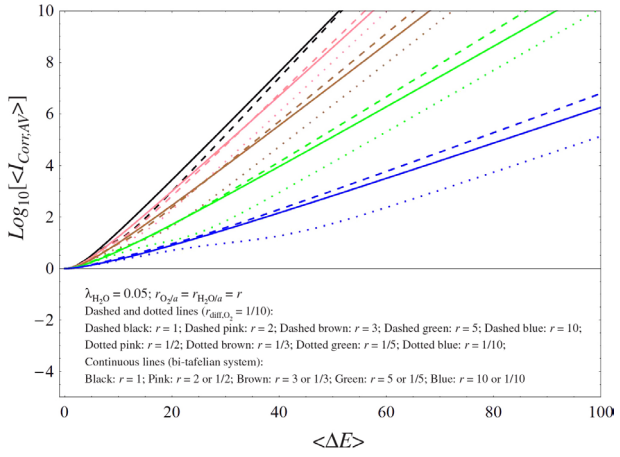

Figure 7. Variation of $<\Delta E_{corr,AV}>$ with respect to <ΔE>. The conditions are the same as those presented in Figure 6. Comparison with a bi-tafelian corrosion mechanism is shown as dashed lines.

In contrast, at high <Δ*E*> values, $<I_{corr,AV}>$ continues to increase, whereas in the absence of the water reduction reaction, this parameter tends to a constant finite limit equal to $1/r_{diff,O_2}$. However, as for $<I_{corr,AV}>$, even if the curves are going closer to the bi-tafelian curves when the second cathodic reduction is involved, these curves do not asymptotically tend to the bi-tafelian case curves with increasing <Δ*E*> value.

Those effects on $<E_{corr,AV}>$ and $<I_{corr,AV}>$ *vs.* <Δ*E*> for the similar system with the three reaction mechanism, but where the contribution of the water reduction reaction λ_{H_2O} is much smaller (λ_{H_2O} = 0.001), are presented in Figures 8 and 9.

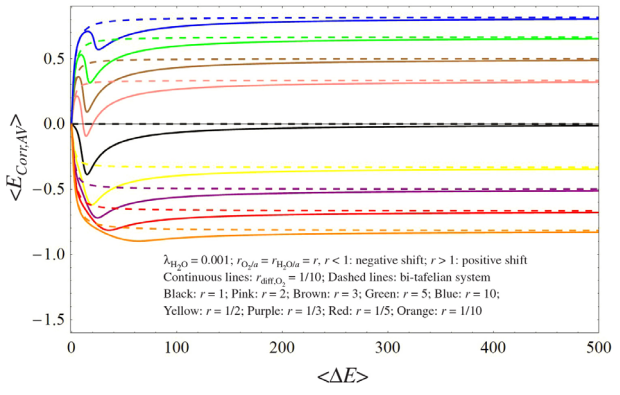

Figure 8. Same as in Figure 6 but with λ_{H_2O} = 0.001.

As for $<E_{corr,AV}>$ with an increasing <Δ*E*> value, even if the curves asymptotically tend towards those calculated

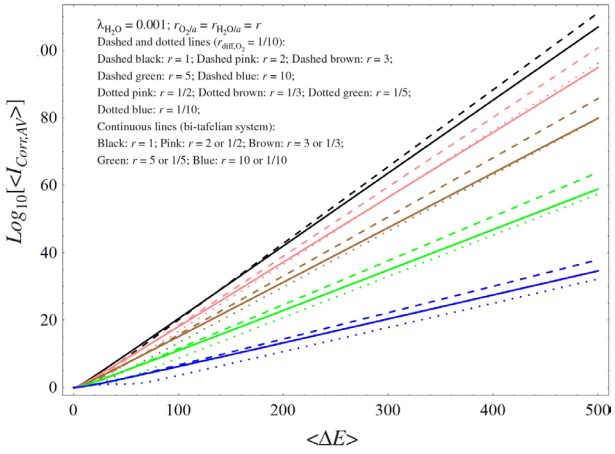

Figure 9. Enhancement of the corrosion current density; the same simulation conditions as in Figure 7, but with λ_{H_2O} = 0.001.

for the bi-tafelian corrosion mechanism, but significantly slower than the case of λ_{H_2O} = 0.05, at high values of <Δ*E*>, beyond 300. Below this threshold value, the potential shift curve is still influenced by the mixed controlled cathodic reaction. As for $<I_{corr,AV}>$, although the effects on the curves are less marked, a similar threshold effect is also observed around <Δ*E*> = 300, between the part of the curve clearly influenced by the mixed controlled cathodic reaction and the part of the curve where the cathodic reaction controlled by the activation energy is dominating.

Even though the water reduction reaction constitutes, in this λ_{H_2O} = 0.001 case, a very minor cathodic process at the near free corrosion potential domain, its influence on the corrosion potential shift at high values of <Δ*E*> is still determining for the overall response to the AC perturbation. This result is readily understood, since in the presence of sufficiently high values of <Δ*E*> whatever the smallness of the λ_{H_2O} value, the exponentially increasing contribution of the activation-controlled reaction dominates the overall cathodic current density.

Effect of the double layer capacitance on the faradaic rectification

In the theoretical analysis presented above, two non-faradaic elements were neglected; the electrolyte resistance R_E and the double layer capacitance C_d. Therefore, the sinusoidal AC perturbation is considered as directly applied to the metal/electrolyte interface. Now, if it is assumed that C_d is independent of the electrode potential and there is no interaction between the two processes, the faradaic and the capacitive one, then the electrochemical interface under consideration can be sketched, cf. in Figure 1b with R_E = 0, as a parallel connexion of a constant double layer capacitance with two faradaic processes.

Since $R_E = 0$, the potential applied at the electrode interface is the AC perturbation potential ($U \equiv E$). The mean current passing across the double layer capacitance for one period of AC perturbation is zero, consequently, the presence of C_d, whatever its value and also independent of the corrosion mechanism considered, does not modify the effect of the faradaic rectification.

Conclusions

Underground steel installations, especially steel pipelines, are generally covered with thick organic coating, and in addition protected cathodically. When these assets are exposed to high AC voltage fields created by high level alternating currents transported by industrial systems in their vicinity, an enhancement of the corrosion may be observed at coating defects, if the CP system is not adequately fitted to this particular electrical constraint. This damaging process, named AC-induced corrosion, is known to originate from the faradaic rectification. This phenomenon, which consists in the modification of the DC mean polarisation curves, including a shift of the DC corrosion potential and an enhancement of the kinetics of the faradaic reactions, when the steel/electrolyte interface is subjected to the stray AC voltage, was studied theoretically.

Faradaic rectification comes basically from the nonlinear character of the current-potential relationship between the faradaic currents and the interfacial potential. It occurs whatever the electrochemical model adopted to simulate the electrochemical behaviour of the interface, this last one being either under pure activation control or under mixed activation-diffusion control. These aspects are largely reported in the literature, for experimental observations as well as theoretical analyses. However, the analysis of AC-induced corrosion when the cathodic current involves two cathodic processes, reduction of dissolved oxygen and that of water under the cathodic protection, as a whole three reaction mechanism for corroding system, as far as we know, is not yet reported. The present work deals with this topic, in such particular, but realistic, situations.

In this first part of the work, the enhancement of the corrosion current density induced by AC voltage perturbation is theoretically derived and digitally simulated. The considerations are here limited to the case where the electrolyte resistance is negligibly small. In this case, the double layer capacitance was assumed to be a pure capacitance (not a constant phase element) and independent of the potential, does not intervene in the faradaic rectification, whatever the model describing the interface behaviour.

The digital simulations of the polarisation curves as well as the results of the analyses of faradaic rectification effect were displayed using dimensionless variables and parameters. Two main dimensionless variables under AC perturbation as output data are the relative corrosion current density enhancement $<I_{corr,AV}>$, i.e., $I_{corr,AV} / I_{corr,0}$, and the relative corrosion potential shift $<E_{corr,AV}>$, i.e., $(E_{corr,AV} - E_{corr,0}) / \Delta E$. They are expressed as a function of the dimensionless AC perturbing amplitude $\Delta E / (R_p I_{corr,0})$. The corrosion kinetic parameters are defined by the several ratios; the anodic and cathodic Tafel constants r ($-b_c / b_a$), the fraction corresponding to the water reduction reaction λ_{H2O} ($-I_{corr,0,H_2O} / I_{corr,0}$) to the overall corrosion current density, the importance of the diffusion limited current density at the corrosion potential without AC perturbation r_{diff,O_2} $[-(1 - \lambda_{H_2O}) I_{corr,0} / I_{lim,O_2}]$. The use of these normalised entities is original, and allowed generalizing the simulation calculations. With such representation it appears that $<E_{corr,AV}>$ and $<I_{corr,AV}>$ are no longer determined by the individual values of b_a and b_c ($= b_{c,,O_2}$, $= b_{c,,H_2O}$) but by their mutual ratio r only.

It was found that when the cathodic reaction is constituted only of the reduction of dissolved oxygen controlled by the mixed diffusion kinetics, whatever the value of r ($r_{O_2/a}$), the relative corrosion potential shift tends to –1 when the amplitude of AC signal increases. In contrast, when the cathodic process is constituted only by the tafelian kinetics or the combination of tafelian and mixed diffusion kinetics, the relative corrosion potential shifts towards cathodic direction when $r < 1$ and towards anodic direction when $r > 1$. When r = 1, there is no change in the corrosion potential whatever the value of ΔE.

For the corroding systems of the bi-tafelian mechanism, when $r > 1$, the relative corrosion potential shifts towards more anodic direction, but to a limited value lower than 1, i.e., absolute shift equal to 100% of ΔE, and depending on the ratio r. Conversely, when $r < 1$ the relative corrosion potential shift decreases from 0 to a limited value greater than –1, equal to that reached by $1 / r$. No dependence of the corrosion potential was observed for $r = 1$ for the bi-tafelian corrosion mechanism.

When the cathodic reaction includes the water reduction reaction, $<I_{corr,AV}>$ tends to infinite when ΔE increases. For sufficiently high ΔE values, $\log(<I_{corr,AV}>)$ *vs.* ΔE curves become linear, that is, the corrosion current density increases exponentially with ΔE. As a whole, the presence of a partial diffusion limitation of the cathodic reaction rate (mixed controlled reaction) significantly decreased the corrosion current enhancement compared with the system of bi-tafelian corrosion mechanism having the same r value.

In an upcoming publication (part II), the case where the electrolyte resistance is no longer negligible will be examined, whereas part III will be devoted to verifications of the model predictions to experimental ones. The effect of the local pH change at the steel/soil interface under AC perturbation and a discussion on how interfacial pH evolution may determine the actual corrosion status of the metal (corrosion protected *vs.* actively corroding) will be presented.

Supplementary Information

Supplementary information is available free of charge at http://jbcs.sbq.org.br as PDF file.

References

1. Kuang, D.; Cheng, Y. F.; *Corros. Sci.* **2014**, *85*, 304.
2. Fu, A. Q.; Cheng, Y. F.; *Can. Metall. Q.* **2012**, *51*, 81.
3. Perdomo, J. J.; Chabica, M. E.; Song, I.; *Corros. Sci.* **2001**, *43*, 515.
4. Cottis, R. A.; Leeds, S. S.; *Corrosion 2009 NACE* **2009**, Product Number 51300-09548-SG.
5. NACE Technical Committee Report; *AC Corrosion State-of-the-Art: Corrosion Rate, Mechanism, and Mitigation Requirements*; NACE Publication Product 35110, Item 24242, 2010.
6. Devay, G.; Szegedi, R.; Labody, I.; *Acta Chim. Hung.* **1964**, *42*, 191.
7. Williams, J.; *Mater. Prot.* **1966**, *5*, 52.
8. Heim, G.; Peez, G.; *GWF, Gas/Erdgas* **1992**, *133*, 3.
9. Jones, D. A.; *Corrosion* **1978**, *34*, 428.
10. Funk, D.; Schoeneich, H.-G.; *3R Int.* **2002**, *41*, 54.
11. Funk, D.; Printz, W.; Schöneich, H.-G.; *3R Int.* **1992**, *31*, 336.
12. Schöeneich, H.-G.; *Oil Gas J.* **2004**, *102*, 56.
13. Ragault, I.; *Corrosion 98 NACE* **1998**, Product Number 51300-98557-SG.
14. Collet, E.; Delores, B.; Gabillard, M.; Ragault, I.; *Anti-Corros. Methods Mater.* **2001**, *48*, 221.
15. Wakelin, R. G.; Gummow, R. A.; Segall, S. M.; *Corrosion 98 NACE* **1998**, Product Number 51300-98565-SG.
16. Di Biase, L.; Cigna, R.; Fumei, O.; *Corrosion 2010 NACE* **2010**, Product Number 51300-10108-SG.
17. Helm, G.; Helm, T.; Heinzen, H.; Schwenk, W.; *3R Int.* **1993**, *32*, 246.
18. Frazier, M. J.; Barlo, T. J.; *Corrosion 96 NACE* **1996**, Product Number 51300-96210-SG.
19. Freiman, L. L.; Yunovich, M.; *Prot. Met.* **1991**, *27*, 437.
20. Nielsen, L. V.; Nielsen, K. V.; Baumgarten, B.; Breuning-Madsen, H.; Cohn, P.; Rosenberg, H.; *Corrosion 2004 NACE* **2004**, Product Number 51300-04211-SG.
21. Pourbaix, A.; Carpentiers, P.; Gregoor, R.; *Mater. Perform.* **2000**, *38*, 34.
22. Funk, D.; Prinz, W; Schöneich, H.-G.; *Ochr. Koroz.* **1993**, *36*, 225.
23. Büchler, M.; *Mater. Corros.* **2012**, *63*, 1181.
24. Büchler, M.; *3R Int.* **2010**, *49*, 342.
25. Büchler, M.; Schöneich, H.-G.; *Corrosion* **2009**, *65*, 578.
26. Yunovich, M.; Thompson, N. G.; *Corrosion 2004 NACE* **2004**, Product Number 51300-04206-SG.
27. Pourbaix, M.; *Atlas of Electrochemical Equilibria in Aqueous Solutions*; NACE International: Houston, 1974.
28. Nielsen, L. V.; *Corrosion 2005 NACE* **2005**, Product Number 51300-05188-SG.
29. Taylor, S. R.; Gileadi, E.; *Corrosion* **1995**, *51*, 664.
30. Hosokawa, Y.; Kajiyama, F.; Nakamura, N.; *Corrosion* **2004**, *60*, 304.
31. Xu, L. Y.; Su, X.; Yin, Z. X.; Tang, Y. H.; Cheng, Y. F.; *Corros. Sci.* **2012**, *61*, 215.
32. Gouda, O. E.; El Dein, A. Z.; El-Gabalawy, M. A. H.; *Electr. Power Syst. Res.* **2013**, *103*, 129.
33. Xu, L. Y.; Su, X.; Cheng, Y. F.; *Corros. Sci.* **2013**, *66*, 263.
34. Tribollet, B.; Meyer, M. In *Underground Pipeline Corrosion*; Orazem, M. E., ed.; Woodhead Publishing: Cambridge, 2014, ch. 2.
35. Jiang, Z.; Du, Y.; Lu, M.; Zhang, Y.; Tang, D.; Dong, L.; *Corros. Sci.* **2014**, *81*, 1.
36. Lazzari, L.; Goidanich, S.; Ormellese, M.; Pedeferri, M.; *Corrosion 2005 NACE* **2005**, Product Number 51300-05189-SG.
37. Ormellese, M.; Lazzari, L.; Goidanich, S.; Sesia, V.; *Corrosion 2008 NACE* **2008**, Product Number 51300-08064-SG.
38. Gellings, P. J.; *Electrochim. Acta* **1962**, *7*, 19.
39. Bertocci, U.; *Corrosion* **1979**, *35*, 211.
40. Lalvani, S. B.; Lin, X.; *Corros. Sci.* **1994**, *36*, 1039.
41. Lalvani, S. B.; Lin, X.; *Corros. Sci.* **1996**, *38*, 1709.
42. Xiao, H.; Lalvani, S. B.; *J. Electrochem. Soc.* **2008**, *155*, C69.
43. Nagy, Z.; Thomas, D.; *J. Electrochem. Soc.* **1986**, *133*, 2013.
44. Bosch, R. W.; Bogaerts, W. F.; *Corros. Sci.* **1998**, *40*, 323.
45. Ibrahim, I.; Takenouti, H.; Tribollet, B.; Campaignolle, X.; Fontaine, S.; France, P.; Schoeneich, H.-G.; *Corrosion 2007 NACE* **2007**, Product Number 51300-07042-SG.
46. Wolfram, S.; *The Mathematica Book*, 5th ed.; Wolfram Media and Cambridge University Press: Champaign, USA and Cambridge, UK, 2003.

Submitted: September 22, 2014
Published online: October 24, 2014